Copyright Warning & Restrictions

The copyright law of the United States (Title 17, United States Code) governs the making of photocopies or other reproductions of copyrighted material.

Under certain conditions specified in the law, libraries and archives are authorized to furnish a photocopy or other reproduction. One of these specified conditions is that the photocopy or reproduction is not to be "used for any purpose other than private study, scholarship, or research." If a, user makes a request for, or later uses, a photocopy or reproduction for purposes in excess of "fair use" that user may be liable for copyright infringement,

This institution reserves the right to refuse to accept a copying order if, in its judgment, fulfillment of the order would involve violation of copyright law.

Please Note: The author retains the copyright while the New Jersey Institute of Technology reserves the right to distribute this thesis or dissertation

Printing note: If you do not wish to print this page, then select "Pages from: first page # to: last page #" on the print dialog screen

Ion Exchanged Glass Waveguides With Efficient Coupling To Fibers And Lasers

SHIQING HU

Abstract: To be of practical use in optical communications networks, optical components must have both low on-chip losses and efficient coupling to fibers, semiconductor lasers and detectors. In this thesis work two types of channel waveguides were designed and fabricated on BK7 glass substrate using a low-cost ion-exchange process. The first type of waveguide was formed in a simple sequence of ion-exchange and post-exchange annealing. These single mode waveguides had large mode size and were efficiently coupled to single mode fibers. The lowest loss achieved in fiber-guide direct coupling was 1.25 dB. The second type of waveguide was formed in a two-step inverse ion-exchange. The single mode waveguides formed in this way had small mode size and were compatible with lasers. The lowest loss achieved in laser-guide butt coupling was around 4 dB. The on-chip mode size transition from laser-compatible to fiber-compatible could be achieved by a thermal tapering annealing step.

APPROVAL PAGE

Ion-exchanged glass waveguide with efficient coupling to fibers and lasers

By

Shiqing Hu

Dr. Janet Lehr Jackel, Bellcore	1-14-92 Date
Dr. Roy H.Cornely Professor of Electrical and Computer Engineering, NJIT	1/13/92 Date
Dr. Haim Grebel Professor of Electrical and Computer Engineering, NJIT	Jan 13, 92 Date

Contents

1. Introduction

2. Design considerations used in this work

3. Fabrication

4. Measurement

5. Experimental results

6. Discussion of results

7. Conclusions and suggestions for future work

8. References

1. Introduction

Recently, glass waveguides have received considerable attention in the development of passive integrated optical components, because of their low cost, low propagation loss and compatibility with optical fibers. The use of photolithographic patterning makes possible the fabrication of complex components on a planar substrate with a few centimeter length. This makes glass waveguide components more attractive over all-fiber components in the employment in optical communications networks if both perform the same function.

There are a large number of approaches to fabricate glass waveguide components. Silica-on-silicon and ion-exchange techniques are two most popular methods.[1] In the first method, the deposited glass waveguide is build up on a substrate which does not form the guide[2]. In the second approach, the glass substrate is modified to make the waveguide. The waveguide formed in this way is imbedded in the substrate.[3-4]

Many glass waveguide components have been realized in laboratories, like interferometric couplers[5], star couplers,[6] wavelength de/multiplexers[7-8] et al. Fig.1-1 shows a star coupler which distributes the light from any input equally into all output channels. A 16 x 16 star coupler has been fabricated on a commercially available glass substrate using ion-exchange technique in Dr. Janet Lehr Jackel's

lab in Bellcore.[9]

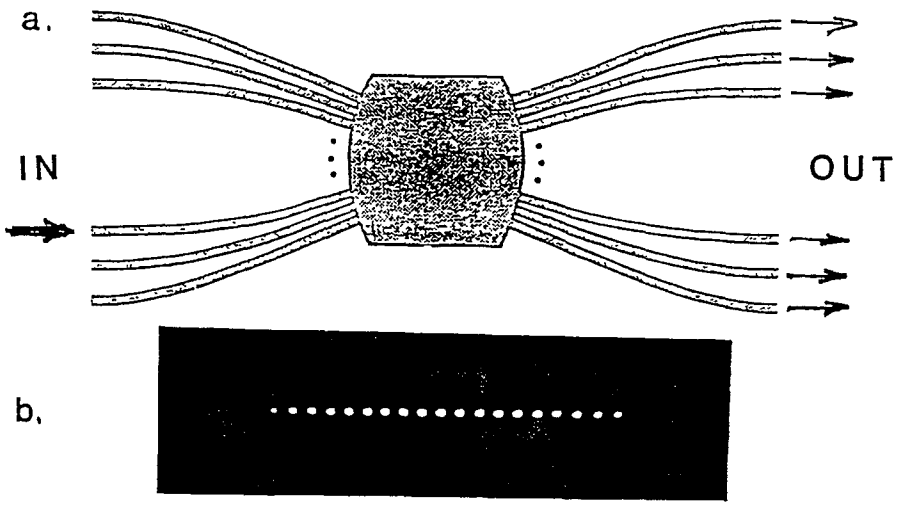

Fig.1-1 A large N x N star coupler. (a) Schematic view.
(b) Distribution of light at exit of such a coupler.
Only one input guide is illuminated.

The practical employment of these optical components in communications networks requires the development of methods of optical packaging. For glass devices, hybrid optical packaging is being developed. Fig.1-2 shows the arrangement in one of this kind of packaging,[10] in which passive components are fabricated on a common glass substrate; optical fibers (or semiconductor lasers) are aligned and directly coupled to the

waveguides using silicon micromachining techniques. [11-12] The silicon chip and the glass substrate can be metallically bounded using flip chip solder bonding technique. [13] This kind of optical packaging allows use of the best combination of optical components to realize the best overall possible system performance.

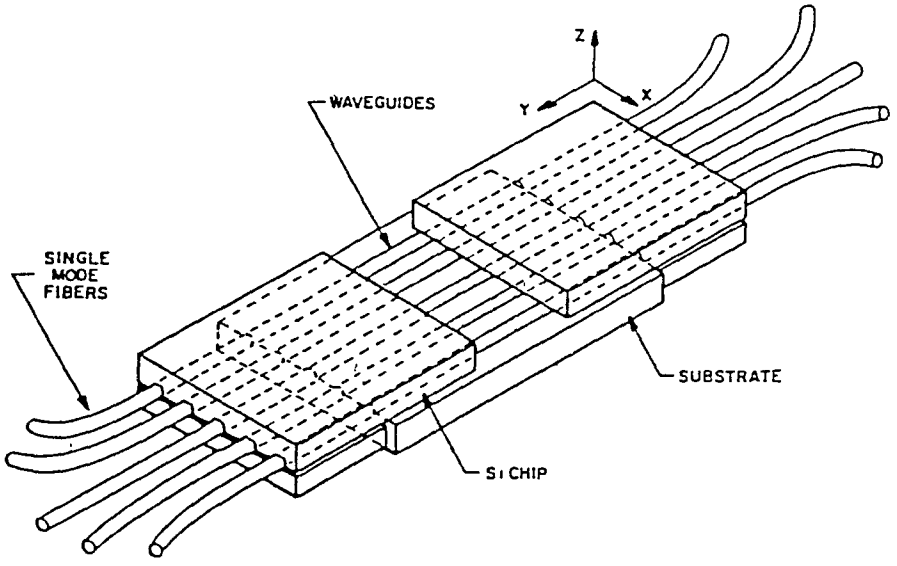

Fig.1-2 An arrangement for obtaining automatic alignment of fiber and waveguide arrays using silicon V-groove lap joints.

One of the challenging engineering issues to be addressed for the hybrid packaging is to develop two types of waveguides on the same glass substrate: one is a "tight mode" waveguide to make efficient butt coupling match to a semiconductor laser;

the other is a "loose mode" waveguide to make efficient butt coupling match to a single mode fiber at optical communication wavelengths, 1.2-1.6 μm. In addition, it is necessary to create low-loss mode size transition from one type of guide to the other.

Low loss laser-compatible waveguide has been realized in silica-on-silicon technology. Charles H Henry et al have reported that a high refractive index single mode nitride rib guide with width of 3 um surrounded by SiO_2 has been fabricated to match the small mode of buried heterostructure semiconductor laser.[14] The reported butt coupling power losses between a laser, operating at 1.52 μm wavelength, and a single mode nitride rib guide and between the same laser and an optical fiber are approximately 4 and 11 dB respectively.

Fiber-compatible channel waveguide has been fabricated on glass substrate using ion-exchange technique. A very encouraging result of 0.28 dB mode size mismatch loss for fiber-guide coupling, and 0.29 dB/cm propagation loss at 1.33 μm wavelength for a silver-sodium exchanged and annealed waveguide has been reported by Huo Zhenguang, Ramakant Srivastava et al.[15]

The mode size tapering can be made geometrically or thermally. Yosi Shani, Charles H Henry et al recently reported that channel waveguides could be adiabatically narrowed and widened by using a geometrical tapering method in one dimension. The reported P-glass waveguide has been tapered from 7 μm wide up to 49 μm wide over a 2 mm length.[16] Mode size tapering has also been reported in ion-exchanged glass waveguides, using thermal tapering. In this method, as reported,[15] only part of the channel waveguide was annealed at the elevated temperature. The mode size of this part of the

channel waveguide increased in both transverse directions after annealing. However, this exchanged and tapered guide was a low index change waveguide (Δn=0.022) which is unsuitable to be used in laser-waveguide coupling. In fact, none of these reports have shown that exchanged waveguides have the capabilities of allowing the transition of the mode size from laser-compatible to fiber-compatible guides with relatively low loss.[17]

This thesis work, during May, 1991 to December, 1991 in BELLCORE, under the advice of Dr. Janet Lehr Jackel has the objective of optimizing the mode size match for semiconductor lasers and fibers. This is a part of a larger optical packaging program, using ion-exchange technology.

In this thesis two alternative methods of ion-exchange waveguide fabrication on glass substrate are presented. Each is designed to form single mode channel waveguides which have efficient coupling to lasers. The first is a single-step silver-sodium ion-exchange process. In this method, a high index change channel waveguide is formed by diffusion of the silver ions from the molten salt into the glass substrate through a photolithographically defined opening in an aluminum mask. The resulting guides couple relatively efficiently to lasers, but couple poorly to fibers because of large mode size mismatch. In the case where fiber-guide coupling is needed, these initially high index change, small mode size guides can be annealed at elevated temperature in order to obtain a large enough mode size for matching a single mode optical fiber. The total loss achieved in fiber-guide coupling for a 2 cm straight waveguide is approximately 1.25 dB operating at 1.53 μm wavelength. Waveguides formed by this method also have the potential to allow the mode size transition from laser-compatible to fiber-compatible with

acceptable loss penalty; preliminary tests of localized annealing have produced smooth transitions from tight modes to large modes.

The second method, an inverse ion-exchange process, is designed to improve coupling of channel waveguides and lasers. The Inverse ion-exchange, originally proposed by P.Pöyhönen et al,[18] is a two-step ion-exchange process. In this work, a high enough index change planar waveguide is fabricated first by regular silver-sodium ion-exchange, then a channel waveguide is formed by outdiffusion of the silver ions from the planar waveguide into the molten salt through photolithographically defined mask openings. A total loss of 4 dB in laser-guide coupling for a 2 cm long waveguide has been achieved. While annealing of these guides to form fiber-compatible mode size has not yet been carried out, it is expected that inverse exchanged guides will respond to annealing in the same way as directly exchanged guides.

2. Design Considerations Used In This Work

2.1 Mode size match consideration.

The mode size and shape are important characteristics of practical devices, because they determine the minimum interface loss between the waveguide and a fiber or the waveguide and a semiconductor laser in butt coupling. The laser used in the experiment is a single quantum well semiconductor laser operating at 1.54 um wavelength with a mode approximately 1.5 - 2.0 μm wide and deep. The optical beam spreads with a half-angle of about 12.5° in both horizontal and vertical directions.[19] The single mode fiber used has a numerical aperture of 0.10-0.11 and a Guassian distribution. The circular mode size of this fiber is approximately 9-10 μm in diameter at the same wavelength.

The accurate mode shape of a channel waveguide could be obtained by solving the wave equation $\mathbf{E} = (\beta^2 - n^2K^2)\mathbf{E}$ in all involved regions. This is significantly difficult, particularly for channels with graded index. The effective index method [20] is often applied to analyze diffused waveguides. In this method the discussion of the mode field is separated into two independent one dimensional problems. The approximation uses effective indices instead of actual indices, therefore, simplifies the problem substantially. A diffused channel waveguide can be, thus, treated as a vertical strong asymmetric planar waveguide and a separate horizontal symmetric planar waveguide, as shown in Fig 2-1.

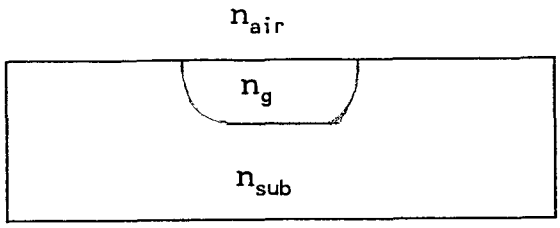

Fig.2-1 Cross-section view of a channel waveguide

According to the solution of a TE wave equation for a planar waveguide with step index change profile, the index difference between the waveguide layer and the substrateΔn which permits a single mode to be excited in a strong asymmetric planar waveguide at a certain wavelength can be determined as:[21]

$$9\lambda^2/32n_f h^2 > \Delta n > \lambda^2/32n_f h^2$$

where λ is the wavelength in free space, n_f is the refractive index of the waveguide layer and h is the thickness of the guide.

To match the mode of the laser (1.5-2μm) or the fiber (9-10μm) used in this experiment, the equivalent step refractive index change (Δn) required for the glass waveguide is estimated roughly in the range of 0.05 - 0.1 and 0.0008-0.007, respectively. The index change for the laser-compatible guide and the fiber-compatible guide is quite different.

2.2 Loss consideration

The correct choice of the refractive index change should be made by taking into account the complete loss of the desired component. The total loss in laser-waveguide-fiber direct coupling shown in Fig.2-2 is the ratio of the laser beam output power to the power launched into the fiber, given in dB.

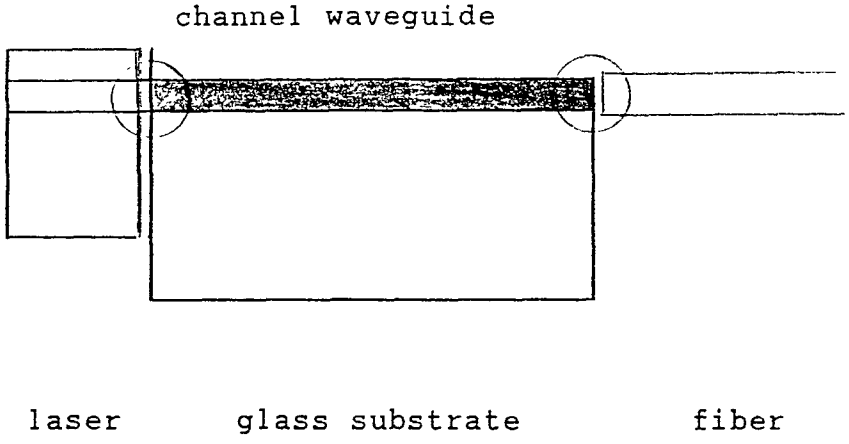

Fig. 2-2 Laser-guide-fiber direct coupling

The constituents of the total loss for a waveguide device in this kind of coupling is explained by Fig.2-2.

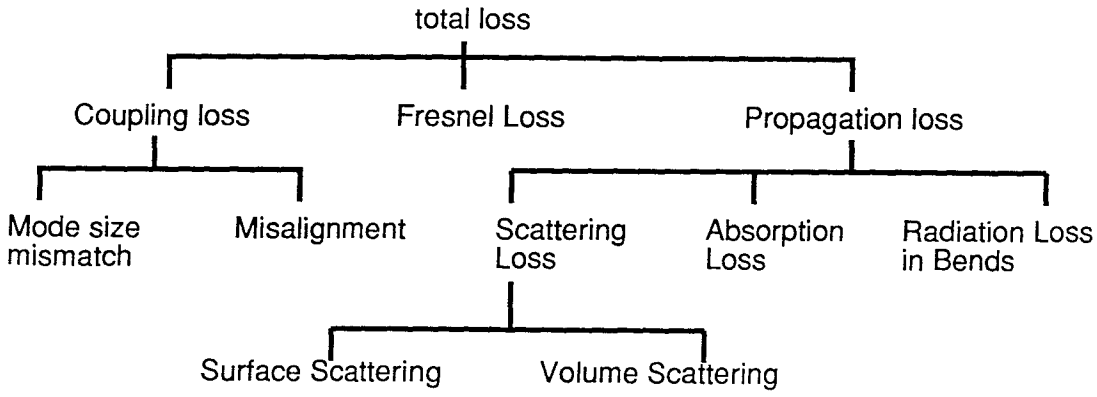

Fig.2-3 The constituents of the total loss.

The losses written boldly in this figure are all directly affected by the refractive index change. To minimize radiation loss, one way is to design bends with large radius of curvature, but that will lengthen the device, resulting in low packing density. The other solution is to develop tight confinement, small mode size waveguides which require a high index change. In contrast, to reduce surface scattering loss, thicker and wider guides with loose confinement are needed.[22] In addition, absorption and volume scattering may be problems for ion exchanged guides with high index. Because of these conflicting requirements, one may choose a moderate value of index change from the allowed range for overall device, or

make waveguides with different mode sizes in different parts of a component.

Some of the devices which will be integrated in the future package have many bends, like star coupler shown in Fig.1-1. In order to obtain efficient coupling between a laser and the waveguide at the input port of the device and to minimize the radiation loss in the bends, high index change was chosen for the waveguides in this work. Surface irregularities were expected to be smoothed out by using a diffusion process, and the need to make the fiber-compatible guides could be solved by a thermal tapering annealing step.

2.3 Considerations of ion exchange process

The BK7 glass slide with constituents shown in Table 2-1 [23] has been chosen as a starting material for the waveguide fabrication. This glass is optically homogeneous and compositionally uniform with refractive index of 1.51 at 0.633 um wavelength. The channel waveguides are fabricated on the glass substrate using ion-exchange. This method is attractive because of the low cost of materials and equipment, flexibility in choosing the numerical aperture and dimension of the guides, simplicity of the process and low loss, high optical quality of formed guides.

Constituent	weight %
SiO_2	68.9
B_2O_3	10.1
Na_2O	8.8
KNO_3	8.4
BaO	2.8
As_2O_3	1.0

Table 2-1 Constituents of BK7 glass: approximate amounts

Ion-exchange in glass involves the exchange of monovalent ions from a molten salt with high mobility ions already in the glass. The sodium ion, for example, is a common constituent of glass. The ions introduced in this way differ from those in glass in ionic size, electronic polarizability, or both. Either case yields optical changes. If a smaller ion from a molten salt replaces a large ion in glass, the glass networks will collapse around the smaller ion, resulting a densely packed structure which has higher refractive index; and if an ion with larger electronic polarizability from a molten salt replaces an ion with small polarizability in glass, the result is an increase in the refractive index, and vice versa. The net change of the refractive index is the result of the combination of these two effects,[3-4] which may have opposite sign.

There are two ions commonly used in exchange: potassium and silver; both give positive refractive index change. However, because of larger difference in ionic size between K^+(1.33Å) and Na^+(0.95Å), K^+ induces greater stress in K^+-Na^+ exchange.[24] As a result, the index change is limited, typically 0.007 for BK7 glass, which is too small to meet the required index change for laser-compatible guides. In addition, stress causes birefringence in the guides, which is unwanted for the desired devices in the optical package. In Ag^+-Na^+ exchange, Ag^+ induces no optical measurable stress because its d-s hybridization outer shell makes it easier to fit into the glass networks.[24] The waveguides formed in this way are nearly polarization independent. The strong interdiffusion between Ag^+ and Na^+ ions results in a large index increase. Consequently, this technique is very promising for the applications that require high numerical aperture and single mode operation, as needed in this work. The index change can be controlled below saturation level by appropriately diluting the silver salts with sodium or/and potassium salts.

Physically, ion-exchange is a thermal diffusion process. For binary exchange this diffusion is characterized by the interdiffusion coefficient D_{in} defined as below:[3]

$$D_{in} = \frac{D_1 D_2 (N_1 + N_2)}{D_1 N_1 + D_2 N_2}$$

where D is the self-diffusion coefficient, N is the ion concentration, and subscripts 1 and 2 refer to the exchanging species. Both inter- and self-diffusion coefficients depends on temperature, activation energy of the exchanging ions, glass

constituents and ionic source concentration. In the limit where one ion is much mobile than the other, the diffusion rate is controlled by the less mobile ion; and where concentrations differ greatly, the diffusion is controlled by the ion with lower concentration.

In Ag^+-Na^+ exchange, the exchange rate is controlled by silver molar fraction in the molten salt once the substrate and the exchanging temperature are chosen. The diffusion profile in the planar waveguide, as well as the index profile in the guide, according to the previous work of Dr. Jackel, is roughly Gaussian. The effective index in the guide approaches different saturation values for different composition of the silver ion source. The depth of the guide can be controlled by exchange time.

3. Fabrication

Two methods of ion-exchange process were used to form waveguides. The first method was a one-step Ag^+-Na^+ exchange. The second method was a two-step inverse exchange. Bk7 glass slides were used as starting material in both methods.

In the first method, a pattern of a set of straight waveguides was first transferred onto the cleaned glass substrate by photolithographic process. The hard contact mode of exposure gave approximate 0.5 μm resolution. After development, the sample was placed in the plasma etch chamber to etch away the residue of the photoresist and the developer. Then a layer of aluminum of 1000 Å was evaporated on the sample in a e-beam evaporator. After lift-off, an aluminum pattern of a set of straight opening strips with width of 3-15 μm was formed on the substrate, which served as the mask in ion-exchange.

The index change in the channel waveguide region was accomplished by Ag^+-Na^+ exchange process. The silver source was a mixture of nitrate salts of $NaNO_3$, KNO_3 and $AgNO_3$ in the molar ratio of 1 : 1 : x, with x ranging from 2-20 %. The melting points of nitrates are lower than other alkali metal salts and the melting point of the mixed nitrates is lower than that of either nitrate in the mixture. This allows the exchange to take place at lower temperature than would otherwise be possible. The ion source was placed in a temperature controlled furnace and all exchanges in the experiment were carried out at $300° \pm 1°c$. An additional purpose of using KNO_3 was to prevent potassium ions in glass from outdiffusing to the

molten salt which would produce microcracks at the glass surface.[24] Before ion-exchange, the aluminum masked glass substrate was pre-heated for a few minutes, it was then immersed in a bath of the molten salts as shown in Fig. 3-1.

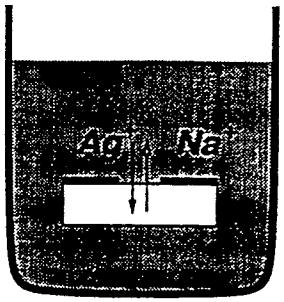

Fig.3-1 Ion exchange is performed by immersing the masked substrate in the molten nitrate salts containing Ag^+.

After exchange for a certain time, the channel waveguides were formed under the mask openings. Then the aluminum mask was removed by etching in phosphoric acid or KOH. The sample was cut to the desired length and two endfaces of the waveguide were polished.

It is very important to have sample with fine edge definition and minimal endface roughness, which would directly affect on the waveguide loss. Hence the polish process is a very important step in waveguide fabrication. The waveguide surface, during the polish, was protected by the polishing blocks which were two glass strips and were mounted on the surface of the guide before the guide was

cut, as shown in Fig.3-2. An epoxy resin with strong edge retention was used for mounting the polishing blocks. Two endfaces of the waveguides were then mechanically polished through several stages ending with 1 micron diamond paste.

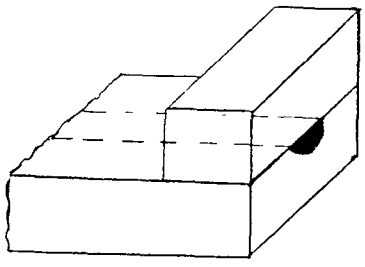

Fig.3-2 Polishing blocks were mounted on the waveguide surface near the end of the guide.

The overall process sequence for one-step exchange is as below and explained as Fig.3-3.

(a) Photolithographically patterning of straight waveguides

(b) E-beam evaporation of Al

(c) Lift-off

(d) Ag^{+}-Na^{+} exchange

(e) Al mask etching

(f) Polish

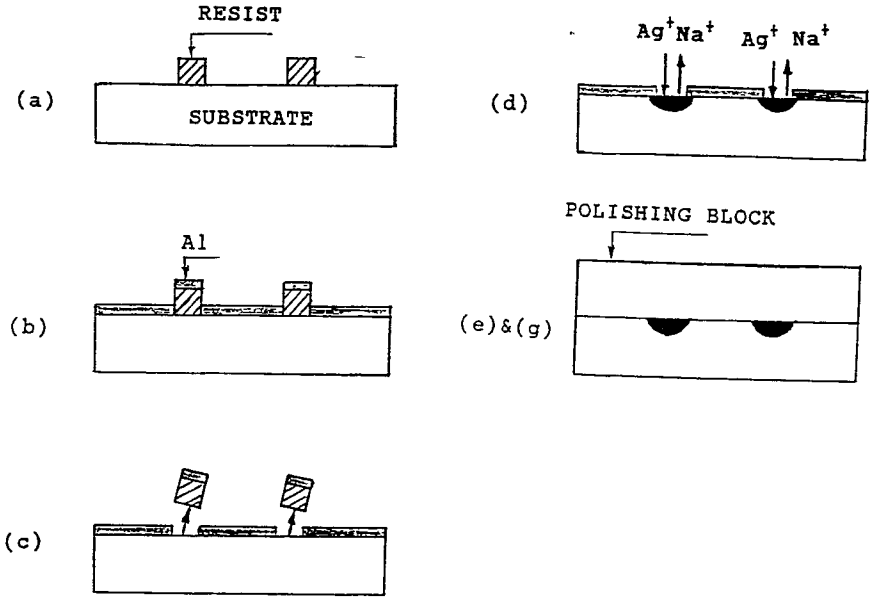

Fig.3-3 Schematic explanation for the formation of a one-step exchanged waveguide.

The second type of waveguide was formed in a two-step ion-exchange. First a planar waveguide was made by diffusing silver ions into an unmasked substrate.

Then an aluminum mask consisting 3-15 μm wide strips was patterned on the substrate. The channels were formed in the second step of ion exchange under the aluminum strips. In this step silver ions outdiffused from the planar guide into the melt through the mask openings. The melt had the composition of 1:1 $NaNO_3$, KNO_3 at 300°c without silver salt. The overall process sequence for this type of the guides is as below, and explained as Fig.3-4.

(a) Ag^+-Na^+ exchange to form planar waveguide

(b) Photolithography

(c) Al evaporation

(d) Lift-off

(e) Ag^+ outdiffusion

(f) Al mask etching

(g) Polish.

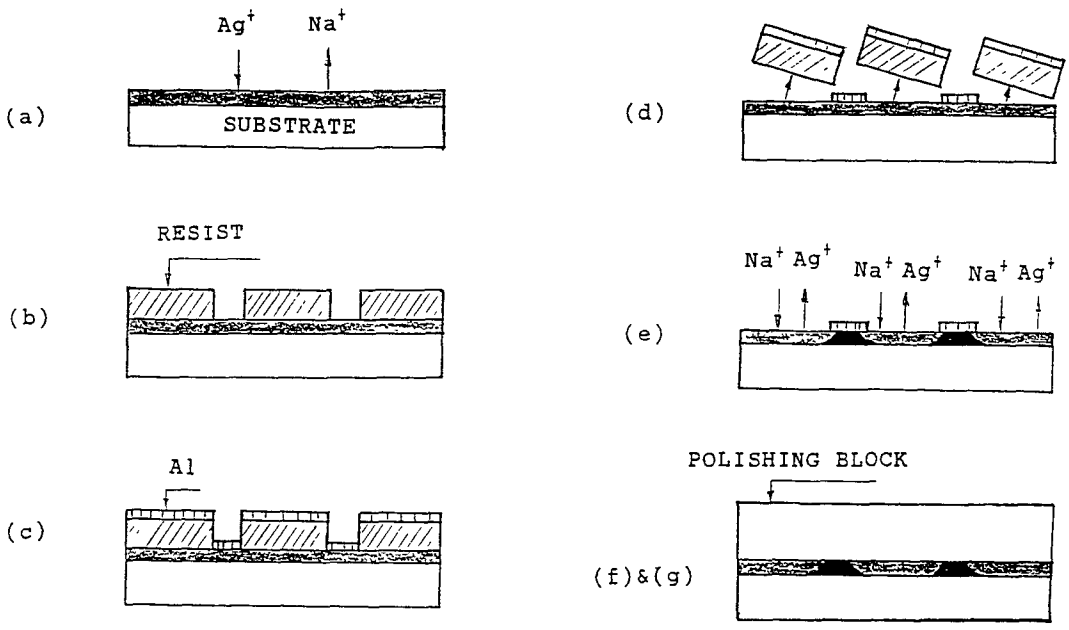

Fig.3-4 Schematic explanation for the formation of a inverse exchanged waveguide.

In the case where guide-fiber coupling is needed these high index change waveguides could be annealed at the elevated temperature. All annealing processes in this work were carried at 400°c with neither melt nor mask present. Localized

annealing or thermal tapering of one end of the waveguide could be done in a specially designed fixture after polish, as shown in Fig.3-5. This fixture heats only about 1 cm at one end of the guide. It consists of an aluminum block containing a slot slightly larger than the waveguide sample; on each side of the slot a cartridge heater is embedded in the aluminum. The temperature of the heater block can be controlled automatically. In this kind of annealing the waveguide sample was straightly inserted into the slot. Only the part which was in the slot was heated. Consequently, the mode size of this part of the waveguide was tapered up to a larger one.

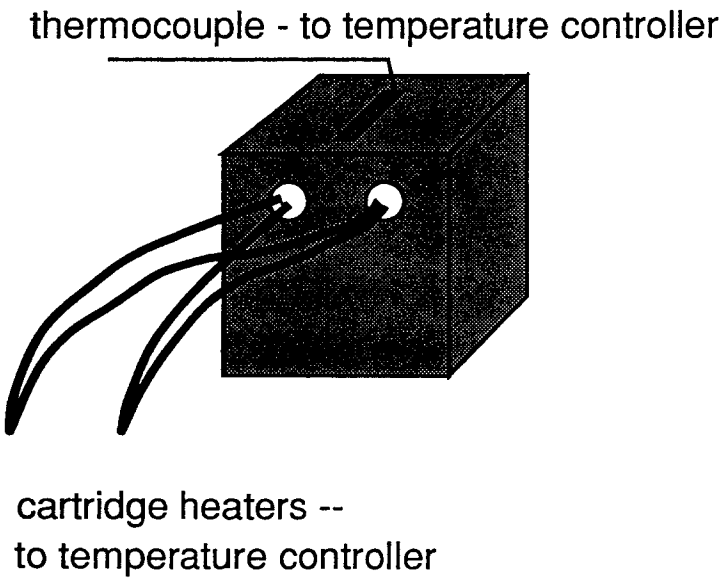

Fig.3-5 The special fixture for thermal tapering of one end of the waveguide.

4. Measurement

The optical characterization of the waveguide was made by two measurements: effective mode index measurement and loss measurement.

Prism coupler technique [25] as used to measure the effective mode indices of the planar waveguides which were ion exchanged under the same conditions as the channel waveguides, but without a mask. This technique is based on the principal of coupled-wave theory.[26] When the light beam is incident from the prism to the prism-air interface, as shown in Fig.4-1, since $n_p > n_a$, it experiences total internal reflection, therefore a standing wave was formed in the x-direction. This standing wave moves in the z-direction with the propagation constant $\beta_p = 2\pi n_p \sin\theta_m/\lambda$. The evanescent tail of this standing wave extends to the air gap between the prism and the planar waveguide. In the planar waveguide, various guided modes can be excited. They all propagate along the waveguide and each guided mode propagates with a corresponding constant β_m. The evanescent tails of these guided mode extend to the air gap also. If the air gap is narrow enough and the light is incident to the prism-air interface at such an angle that $\beta_p = \beta_m$, the optical energy of the standing wave in the prism can be coupled to the mth-order mode of the waveguide through the overlapping evanescent tails.

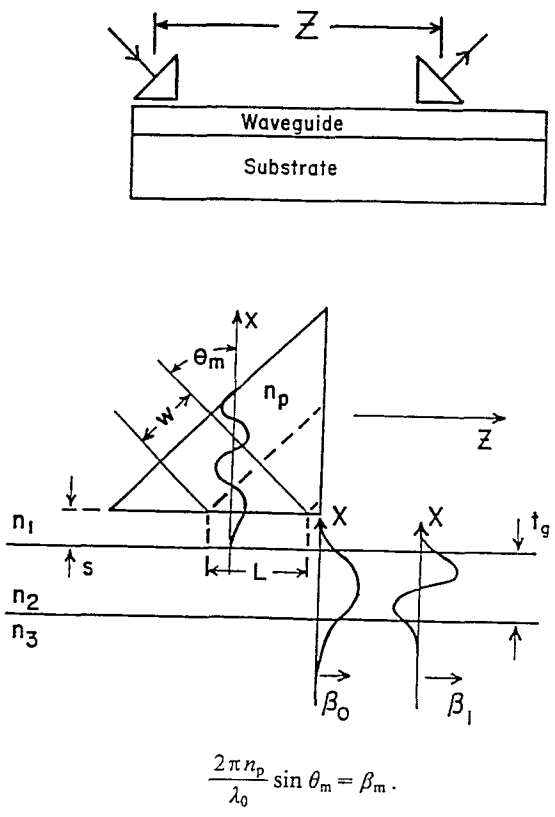

$$\frac{2\pi n_p}{\lambda_0}\sin\theta_m = \beta_m .$$

Fig.4-1 Diagram of a prism coupler. The electric field distributions of the prism mode and the m=0 and m=1 waveguide modes in the x direction are shown.

In the measurement the light was launched from a helium-neon laser operating at 0.633 μm to the input prism. By changing the incident angle gradually a set of intensity maxima could be found at the output, which correspond to a set

of selectively excited modes. The effective mode index N was then calculated as

$$N = n_p \sin [A + \sin^{-1} (\sin \underline{i} / n_p)]$$

where n_p was the refractive index of the prism, A was the angle between incident face and the prism base, and $\underline{i}$ was the coupling angle at which a intensity maximum was observed at the output. The accuracy of the effective index measurement in this work was about 10^{-3}. The details about this measurement and the set-up can be found in Reference 25.

From the set of measured effective mode indices and the index of the glass substrate, the vertical refractive index profile of the planar waveguide and its surface value were recovered by use of the inverse WKB method [27], which was programmed. The diffusion depth and the effective diffusion coefficient were then measured and calculated from the reconstructed profile. Fig.4-2 shows a reconstructed index profile, as an example. In this profile the surface index is measured as 1.5324. The index of the substrate is known as 1.5168. The index difference between the surface of the guide and the substrate Δn is 0.0156. The depth of the guide is defined as the depth at which the index increase equals 1/e of Δn. From the profile the depth is found as 6.13 μm.

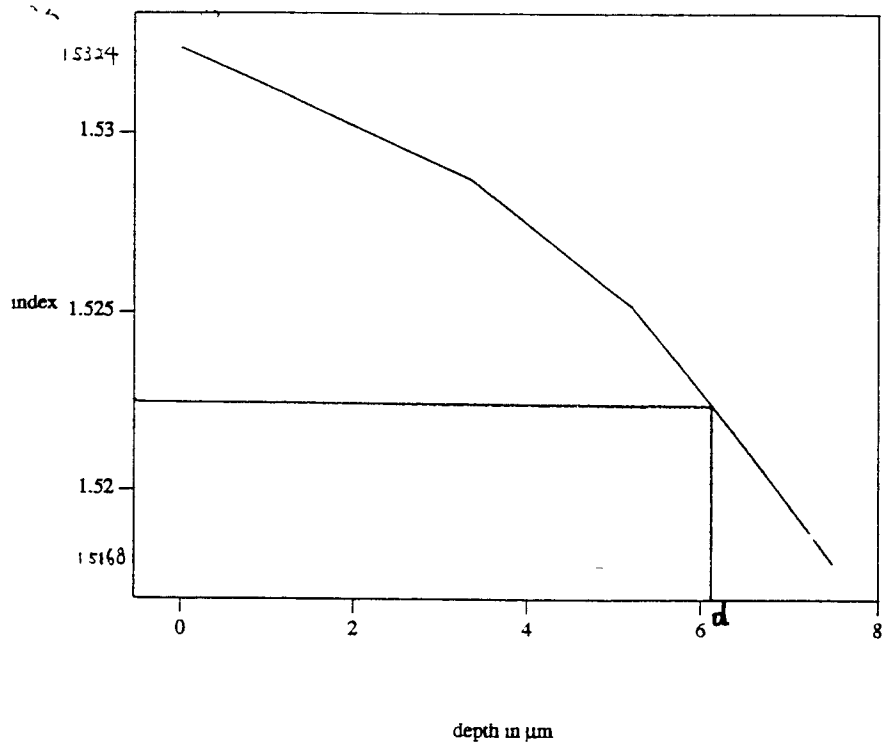

Fig.4-2 Index profile reconstructed by the inverse WKB method.

All the loss measurements described below were made using direct coupling: a fiber or laser was brought nearly into contact with the polished end of the waveguide. No lenses, AR coatings, or index matching materials were used. In fiber-guide and laser-guide coupling measurements, the output face of the guide was imaged onto a detector using a microscope objective with a large enough numerical aperture (0.57) to capture all the light. The set up for the loss measurement was shown in Fig.4-3.

The fiber, the waveguide sample and the microscope objective were mounted on the individual precision translation stage which allows for X, Y, Z

adjustments. The uncertainty for loss measurement was mainly caused by misalignment, especially angular misalignment between the two endfaces, therefore piezoelectrically driven micrometer heads and angular adjustment were used for the alignment equipment in this work.

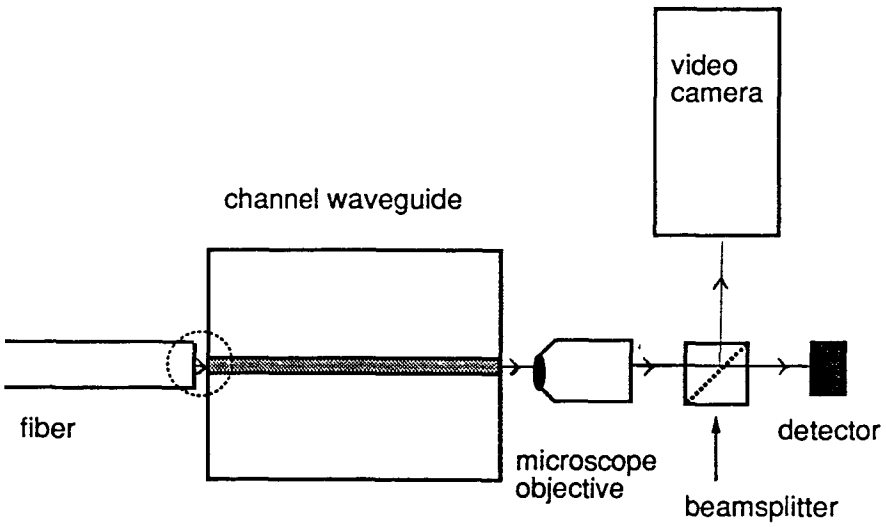

Fiber-to-Waveguide Coupling

Fig.4-3 The set-up for loss measurement

Coarse alignment of the fiber to the guide or laser to the guide was facilitated by observing the output image using an IR video camera. Only if the outface image the channel waveguide, which was a well confined light spot was found on the screen, the output of the waveguide could be imaged onto a Ge detector. There was a small aperture just placed before the detector to reject the

scattering light. The fine alignment first was made in both transverse direction to achieve the peak power, then the pigtail of the fiber was moved along the longitudinal axis until a maximum occurs. The spacing between the endfaces was minimized in this way, therefore the uncertainty caused by Fresnel reflection and Fabry-Perot interferometer effect were minimized. By carefully alignment the deviation of a few tenth dB for the same waveguide in loss measurement could be achieved.

The output power of the semiconductor laser or the fiber was measured before and after the coupling in order to determine the possible drift, a 2-3% power drift was once found in the output power of the fiber.

The entire loss measurement procedure is summarized as below:

(a) Make coarse alignment and view output of the waveguide on the screen of the video monitor.

(b) Determine the single mode region over the width of the mask opening by observing the profile of the mode field for each waveguide.
(Additional video hardware is available for this need.)

(c) Make fine alignment and measure the output intensity of the waveguide.

(d) Take away the waveguide and move the fiber or laser towards the microscope objective until a focused the image was found on the screen and measure the power.

More details about the loss measurement can be found in Reference 28.[28]

5. Experimental Results

Fig.5-1 shows the measured index changes and the effective diffusion coefficients for different composition of the silver source. The index change Δn in the figure is defined as the index difference between the surface of the planar guide and the substrate. The effective diffusion coefficient D_{eff} is defined as $d(n_{sub} + \Delta n/2) = \sqrt{D_{eff} t}$, where t is time.

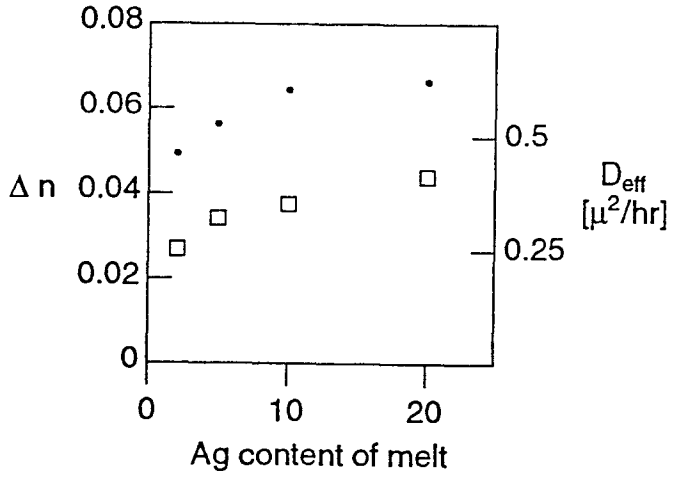

Fig.5-1 Index change (•) and effective diffusion coefficient (□)
as a function of melt composition for BK7 glass, T = 300°c.

THe total loss for these one-step exchanged guides in laser-guide coupling has been measured. The losses for the guides exchanged for 2 and 4 hours in 5% $AgNO_3$ melt, and 2 hours in 20% melt are shown in Fig.5-2. For the sample exchanged for 4 hours, all but 3 μm wide guide are double moded. The loss shown in the Fig.5-2 is the loss coupling to the fundamental mode in the wider guide. For

the samples exchanged for 2 hours, all guides shown are single moded. The mask opening, given in the figure, defines the width of the channel waveguide, never the less, the final width of the waveguide depends on the diffusion parameters.

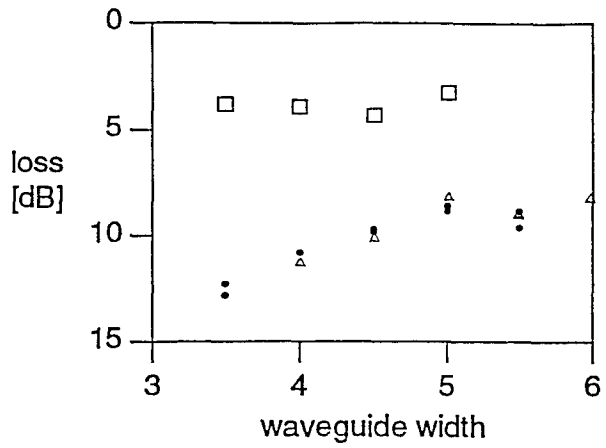

Fig.5-2 Loss for laser-waveguide coupling including 3 cm propagation loss in waveguides, exchanged (•) 2 hr, (□) 4 hr in 5% $AgNO_3$ melt, (▲) 2 hr in 20% $AgNO_3$ melt.

The total loss of 4 dB for these 4-hour one-step exchanged guides compares favorably with 10% coupling typically achieved in laser-fiber butt coupling.

The measured total losses for the one-step exchanged and annealed waveguides in fiber-guide coupling are shown in Fig.5-3, the guides were silver-exchanged for 2 hours in 5% $AgNO_3$ melt, then annealed for 2 and 3 hours. It can be seen that the loss is significantly reduced after annealing. More information about annealing is summarized in Table 5-1, where the diffusion depth d is defined

as the depth at which the refractive index $n(d) = n_{sub} + \Delta n/e$. The comparison of the loss for the waveguide with the mask opening of 5 um for different annealing time is also shown in the table. The best result for the total loss is approximately 1.25 dB for a 2 cm long waveguide with the mask opening of 5 um. A similar result has been achieved for the guides exchanged for 3 hours in 5% $AgNO_3$ and then annealed.

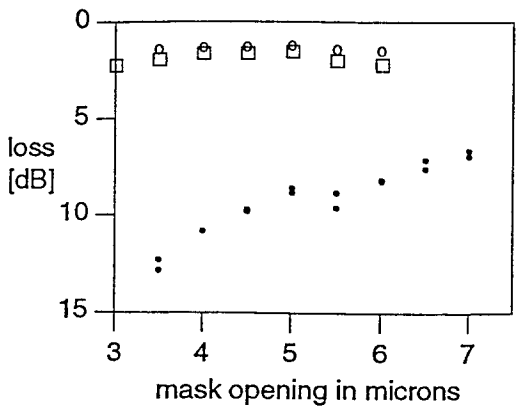

Fig.5-3 Loss for the waveguides exchanged 2 hours in 5% $AgNO_3$ melt, as-exchanged (•), annealed (□) for 2 hr at 400°c, and annealed (o) 3 hr.

annealing time (hr)	single mode region of w_m (μm)	depth (μm)	total loss for w_m=5μm (dB)
0	3.0-5.5	2.0	6.30
1	3.0-5.5	5.3	3.54
2	3.0-6.0	6.2	1.59
3	3.0-6.0	7.8	1.25

Table 5-1 The comparison of the waveguides for different annealing time.

The total loss for these guides in fiber-guide-fiber coupling was also measured. In this measurement a single mode fiber was brought to the output endface of the waveguide to collect the light. The measured fiber-guide-fiber losses for the set of the guides initially exchanged for 2 hours and then annealed for 3 hour are shown in Fig.5-4, along with the fiber-guide loss. This loss is defined as the excess over one fiber-to-fiber direct connection.

Fig.5-5 shows the output image of an inverse exchanged channel waveguide in laser-guide end-butt coupling. The photograph was taken from the IR video monitor. This guide was formed under 3 um wide aluminum strip in 30-minute outdiffusion from an initially 3-hour Ag^+-Na^+ exchanged planar waveguide.

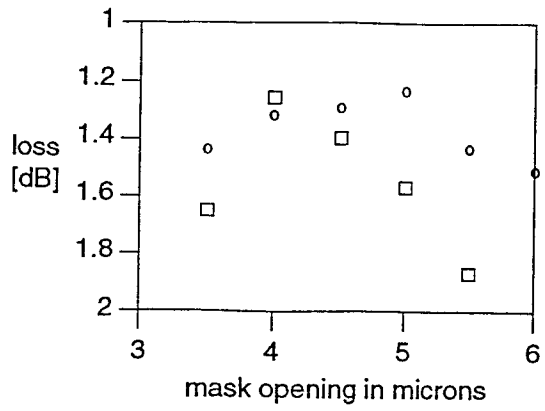

Fig.5-4 Loss for fiber-guide-fiber coupling (□) compared with fiber-guide coupling(o) for the same set of guides: 2 hr ex. 3 hr ann.

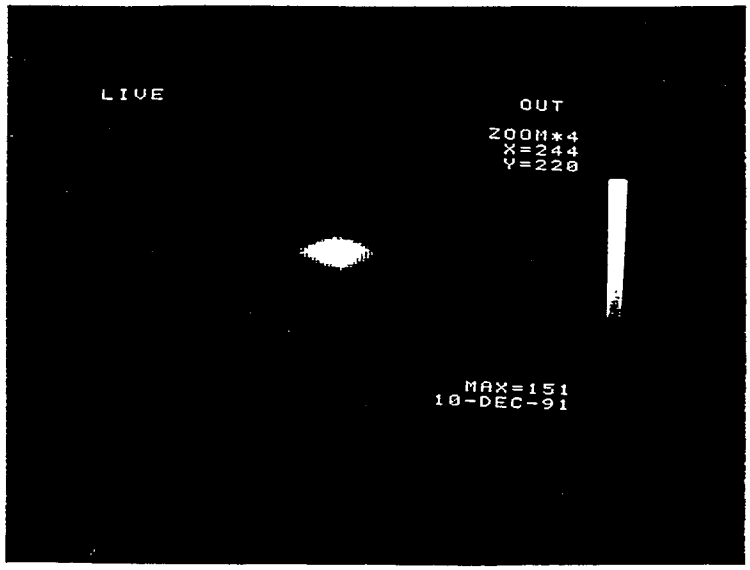

Fig.5-5 The output image of 3 μm wide inverse exchanged channel waveguide: 3 hour original exchange, 30 minute outdiffusion.

Fig.5-6 shows the total loss in laser-guide coupling for 2 cm long two-step inverse exchanged channel waveguides with 2-hour original planar exchange and 30-minute outdiffusion. The loss for the 2-hour one-step exchanged guides in laser-guide coupling is also shown in Fig.5-6 as comparison.

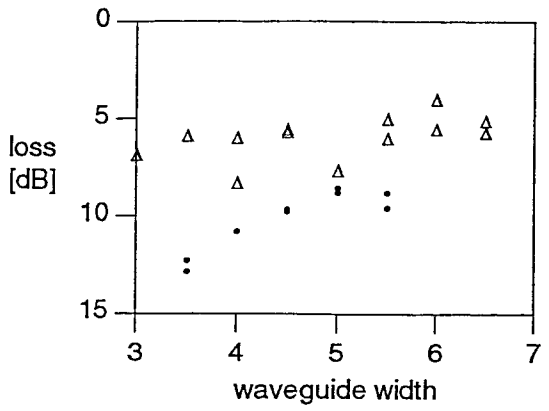

Fig.5-6 Loss for the inverse exchanged guides in laser-guide coupling comparing 2 hour single-step (•) and two-step (Δ) exchange with 2 hour planar exchange and 30 minute outdiffusion.

Thermal tapering annealing for one end of the guide is in progress. Measured effective mode indices as a function of the position along the taper is shown in Fig.5-7. The data show that the a smooth index variation along the taper has been achieved.

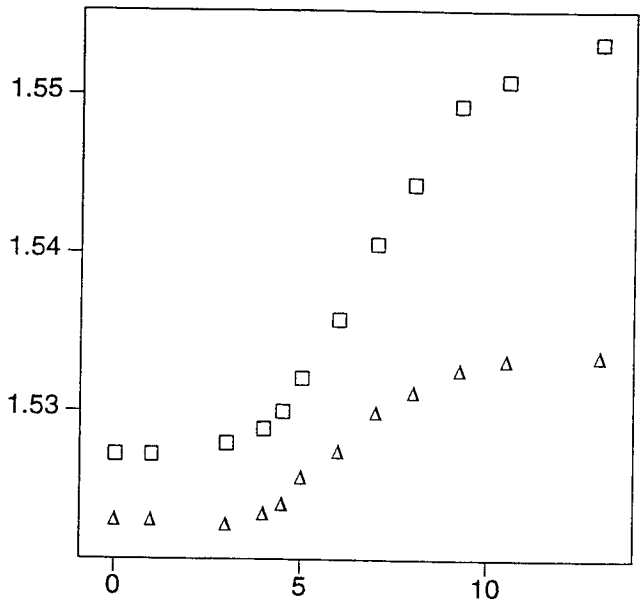

Fig.5-7 Measured mode indices as a function of the position along a guide (in mm) exchanged 2 hr. in 20% Ag mix. and annealed 1 hr. at 400°c in the heater block shown in Fig.3-5.

6. Discussion Of Results

As described in section 2, mode size mismatch loss and scattering loss are related to the guide index, refer to Fig.2-2. The significant reduction of the loss in fiber-guide coupling for annealed guides is attributable to the further indiffusion of the silver ions in both transverse directions of the channel waveguides. This diffusion affects the loss in three ways. First, this diffusion increases the waveguide mode size and pushes the index peak further into the substrate. This makes the waveguide mode more nearly circularly symmetric, resulting in a substantial improvement of the mode shape overlap between the fiber and the waveguide. As can be seen in Table 5-1, the depth of the guide increased to approximate 8 μm after 3-hour annealing, which is very close to the fiber mode size. Second, the changes in the mode size and the surface index also reduce surface scattering since the guided light in the wider and deeper guides experiences less interaction with the surface and the sides of the guide. The third reason for the loss reduction is the decrease of the silver ion concentration in the waveguides, thus any volume scattering or absorption caused by high silver concentration is reduced.

It is interesting to notice that the dependence of the loss on the mask opening becomes less sensitive for the annealed guides. The deviation of the loss for the set of 3-hours annealed guides (3.5-6.0 μm) is only 0.26 dB as comparison with 4-5 dB for the same set of guides without annealing, as seen in Fig.5-3. The possible reason for this difference may relate to the side diffusion. The guides formed by one-step exchange are still shallow surface guides. Mode width depends

primarily on the width of the mask opening, rather than on side diffusion. The relative consistency of the loss shown in the annealed guides indicates the relative consistency of the mode size. This implies that the significant side diffusion occurs in long time annealing, which makes mode width less dependent on the initial mask opening.

The total loss around 4 dB for the high index change waveguide formed in both ion-exchange methods shows these guides can be efficiently coupled to lasers. The desired index change for laser-compatible guides, as designed in section 2, is around 0.06-0.07. It can be seen, from Fig.5-1, that 10-20% $AgNO_3$ may give the best match to this requirement. Comparing the loss for the guides exchanged for 2 hours in 5% and 20% $AgNO_3$ melt, one can find no large reduction of the loss for the guides exchanged in 20% $AgNO_3$ melt. The reason for this, we believe, is that the better mode size match may be achieved at the expense of greater propagation loss which is caused by high silver concentration in the guide.

Side diffusion in the two methods of ion-exchange affects the mode width in different way. In one-step exchange side diffusion always tends to widen the channel, as shown in Fig.3-3 (d). While in inverse exchange process, side diffusion tends to narrow the channel as shown in Fig.3-4 (e). In addition the inward and outward diffusion of the silver ions shift the index peak below the surface yielding a buried symmetric guide. This second exchange offers similar advantages to annealing in terms of the improvement of the mode shape and the reduction of scattering, but instead of giving a wider mode, it results in a narrower mode.

Consequently, better coupling between laser and the guide is expected. The data shown in Fig.5-6 demonstrate the advantage of this two-step inverse exchange.

The exchange time in the second step inverse exchange is very critical in the formation of the channel. Shorter and longer exchange time all cause poor lateral confinement. The poor lateral confinement in longer exchange time corresponds to too small index difference at the surface between the masked area and its adjacent open area. This is caused by silver ions under the mask diffusing too far down into the substrate. In the experiment, among three planar waveguides which were exchanged for 2 hours in 5% $AgNO_3$ melt, the channels were only formed in the masked planar guide with 30-minute outdiffusion. The 15-and 60-minute outdiffusions did not provide good lateral confinement, consequently, these two samples still acted as planar waveguides.

7. Conclusions And Suggestions for Future Work

Two classes of high index waveguides needed in laser-guide and fiber-guide coupling were realized in BK7 glass substrate using Ag^+-Na^+ exchange. The process conditions were studied in detail. The optical characterization of the waveguides were used to facilitate the optimization of the exchange conditions. The lowest fiber-guide coupling loss of 1.25 dB was achieved for a 2 cm long single mode channel waveguide which was formed by one-step Ag^+-Na^+ exchange in 5% $AgNO_3$ melt for 2 hours at 300°c, followed by thermal annealing for 4 hours at 400°c. A total laser-guide coupling loss of 4 dB was achieved either by one-step exchange in 5% $AgNO_3$ for 4 hours at 300°c or by planar exchange in 5% $AgNO_3$ melt for 2 hours followed by 30-minute outdiffusion at the same temperature. The results show these high index waveguides may be ideal candidates for fabrication of IOC with large packing density and with semiconductor lasers as input power. Preliminary work on thermal tapering at one end of the guide was made. The results indicates that the output end of the device can be thermally tapered using the same annealing time at the same temperature in a specially designed fixture so that only one end of the guide is heated. The mode size of the channel waveguide, therefore, can transit from laser-compatible to fiber-couple.

For future work to improve guide fabrication, it is felt that theoretical modeling in two aspects would be useful for this research: (a) side diffusion in thermal annealing and (b) the silver concentration profile in the inverse exchanged waveguide. It is also suggested that SEM analyze could be used to determine the

silver concentration in the channel waveguide.[29]

8. References

1. Janel L. Jackel, "Glass waveguide components-an overview", (internal), 1991, Bellcore.
2. C. H. Henry, G. E. Blonder and R. F. Kazarinov, "Glass waveguides on silicon for hybrid optical packaging", J. Lightwave Technol., Vol.7, 1530-1539, (1989).2.
3. T Findakly "Glass waveguides by ion exchange: a review," Optical Engineering, Vol. 24, No. 2, 244-250, (1985).
4. R. V. Ramaswamy, "Ion-exchange glass waveguides: a review", IEEE/OSA J. Lightwave Technol. LT-6, 984-1002, (1988).
5. H. Kogelnik and R. V. Schmidt, "Switched directional couplers with alternating ", IEEE J. Quantum Electron, QE-12, 396-401, (1976).
6. C. Dragone, "Efficient N x N star couplers using Fourier optics", J. Lightwave Technol. Vol 7, No. 3 479-489, (1989).
7. Arjen r. Vellekoop and Meint K. Smit, "Four-channel integrated-optic wavelength demultiplexer with weak polarization dependence", J. Lightwave Technol. Vol 9, No.3, (1991).
8. H. Takahashi, S. Suzuki, I. Nishi, "Multi/demultiplexer for nanometer-spacing WDM using arrayed-waveguide grating", Topical Meeting on Integrated Photonics Research, Paper PD-1, Monterey CA, 1991.
9. J. L. Jackel, S. Q. Hu and J. J. Johnson, "Wavelength and polarization independent 16x16 star coupler fabricated using ion exchange in glass", (unpublished), 1991.
10. E. J. Murphy and T. C. Rice, "Self alignment techniques for fiber attachment to

guided wave devices", IEEE J. Quantum Electron, QE-22(6), P.928, (1986).

11. C. Edge, M J Wale, F A Randle and D J Pedder, "Robust interfacing of integrated optics with optical fibers using a self-aligning technique", (internal).
12. Peterson, "Silicon as mechanical material", Proceeding of the IEEE, Vol 70, No. 5, 42-48, (1982)
13. D. J. Pedder, "Flip chip solder bonding for microelectronic application", Hybrid Circuits, No.15, 4-7, (1988).
14. As reference 2, p.1553.
15. Huo Zhengguang, Ramakant Srivastava, and Ramu V. Ramaswamy, "Low-loss small-mode Passive waveguides and near-adiabatic tapers in BK7 glass," J. Lightwave Technol. 7, 1590-1595, (1989).
16. Yosi Shani, Charles H. Henry, Rodney C. Kistler, Rudiloph F. Kazarinov, and Kenneth J. Orlowsky, "Integrated optic adiabatic devices on silicon," IEEE J. Quantum Electron, 27, 556-566, (1991).
17. As reference 16, P.564.
18. P. Pöyhönen, S. Houkanen, and A. Tervonen, "Inverse ion-exchange method for glass waveguide fabrication," Optics Letters, Vol.15, No.21 1206-1208, (1990).
19. C. E. Zah, R. Bhat, B. Paithak, C. Caneau, F. J. Favir, N. C. Andreadakis, D. M. Hwang, M.A. Koza, C. Y. Chen, and T.P. Lee, "Low threshold 1.5 um tensile-strained single quantum well laser", Electron, Lett, 27, 1414-1415, (1991).
20. T.Tamir, "Topics in applied physics: Integrated optics," Vol.7 64-66.
21. R. G. Hunsperger "Integrated optics: Theory and technology," second edition, 36-37.
22. As reference 21, Chapter 5.

23. BK7 data, Schott, 1991.

24. C De Bernardi, S. Morasca, D. Scarano, A. Carnera and M.Morra, "Compositional and stress-optical effects in glass waveguides: comparison between K-Na and Ag-Na ion exchange", J. Non-Crystalline Solids 119 195-204, (1990), North-Holland.

25. As reference 20, P. 222-223.

26. As reference 21, P. 94-96.

27. White and P. F. Heidrich, "Optical waveguide refractive index profiles determined by measurement of mode indices: a single analysis", J. Applied Optics, Vol. 15, No. 1, 151-155,1976.

28. Dan Courtney, Tim Bailey, "Optical characterization of integrated optical devices", SPIE Vol. 835 Integrated Optical Circuit Engineering, 218-228, (1987).

29. P. C. Noutsios and G. L. Yip, "Shallow buried waveguides made by purely thermal migration of K^+ ions in glass", SPIE Vol. 1177 Integrated Optics and Optoelectronics, 2-7, (1989).